

Inorganic nitrogen transformations in the bed of the Shingobee River, Minnesota: Integrating hydrologic and biological processes using sediment perfusion cores

*Richard W. Sheibley*¹

Department of Chemical Engineering, University of California, Davis, California 95616

John H. Duff

U.S. Geological Survey, Menlo Park, California 94025

Alan P. Jackman

Department of Chemical Engineering, University of California, Davis, California 95616

Frank J. Triska

U.S. Geological Survey, Menlo Park, California 94025

Abstract

Inorganic N transformations were examined in streambed sediments from the Shingobee River using sediment perfusion cores. The experimental design simulated groundwater–stream water mixing within sediment cores, which provided a well-defined one-dimensional representation of in situ hydrologic conditions. Two distinct hydrologic and chemical settings were preserved in the sediment cores: the lowermost sediments, perfused with groundwater, remained anaerobic during the incubations, whereas the uppermost sediments, perfused with oxic water pumped from the overlying water column, simulated stream water penetration into the bed. The maintenance of oxic and anoxic zones formed a biologically active aerobic-anaerobic interface. Ammonium (NH_4^+) dissolved in groundwater was transported conservatively through the lower core zone but was removed as it mixed with aerated recycle water. Concurrently, a small quantity of nitrate (NO_3^-) equaling ~25% of the NH_4^+ loss was produced in the upper sediments. The NH_4^+ and NO_3^- profiles in the uppermost sediments resulted from coupled nitrification-denitrification, because assimilation and sorption were negligible. We hypothesize that anaerobic microsites within the aerated upper sediments supported denitrification. Rates of nitrification and denitrification in the perfusion cores ranged 42–209 and 53–160 $\text{mg N m}^{-2} \text{ day}^{-1}$, respectively. The use of modified perfusion cores permitted the identification and quantification of N transformations and verified process control by surface water exchange into the shallow hyporheic zone of the Shingobee River.

Nitrogen transformations in soil and sediments have been a focus of research for many years, with nitrification and denitrification most commonly studied. When these reactions co-occur, the result is a net loss of N that can have significant biological consequences in both aquatic and terrestrial systems. The capacity of stream beds to process N has been an area of recent interest, especially in the midwestern United States, where high nitrate (NO_3^-) in agricultural runoff has been implicated as a cause of hypoxia in the Gulf of Mexico (Turner and Rabalais 1994).

Nitrification and denitrification studies have most commonly involved the use of enzyme assays with sediment slurries, revealing “potential” reaction rates (Rysgaard et al.

1994; Strauss and Lamberti 2000). Potential rates represent the optimal rate resulting from substrate enrichment. Sediment profiles are destroyed, promoting substrate diffusion, the loss of natural chemical gradients, and disruption of microbial aggregates (Killham 1994; Garcia-Ruiz et al. 1998). These disturbances enhance microbial activity and increase process rates (Marxsen and Fiebig 1993). As a result, slurry incubations are more useful in a comparative context than as estimates of in situ activity.

Soil and sediment perfusion cores have been used to study in situ nitrification and denitrification kinetics over the past three decades. Disturbance of the sediment structure is minimized, and the natural chemical gradients and biomass distribution are preserved (Ardankani et al. 1974; Marxsen and Fiebig 1993). Intact cores also maintain hydrologic characteristics that reflect in situ rates of diffusion, dispersion, and advection, all of which influence biological reactions. In general, sediment cores provide a quasi realistic simulation of natural sediment processes in lakes, estuaries, and coastal oceans (Nishio et al. 1982).

Groundwater and surface water interactions in the hyporheic zone can greatly influence nutrient processing in streams (Triska et al. 1989; Grimm 1996; Duff and Triska 2000). Although the development of the hyporheic zone con-

¹ Present address: Department of Biology, Arizona State University, Tempe, Arizona 85287 (rwsheibley@asu.edu).

Acknowledgments

We gratefully acknowledge funding provided by NSF grant DEB 94-20282 and the U.S. Geological Survey National Research Program. We thank S. A. Thomas, M. J. Kemp, and two anonymous reviewers for a thorough critique of our manuscript. We also thank Jeanne DiLeo for formatting the graphics. Any citation of a specific product by brand name is for descriptive purposes only and does not constitute endorsement by the U.S. Geological Survey.

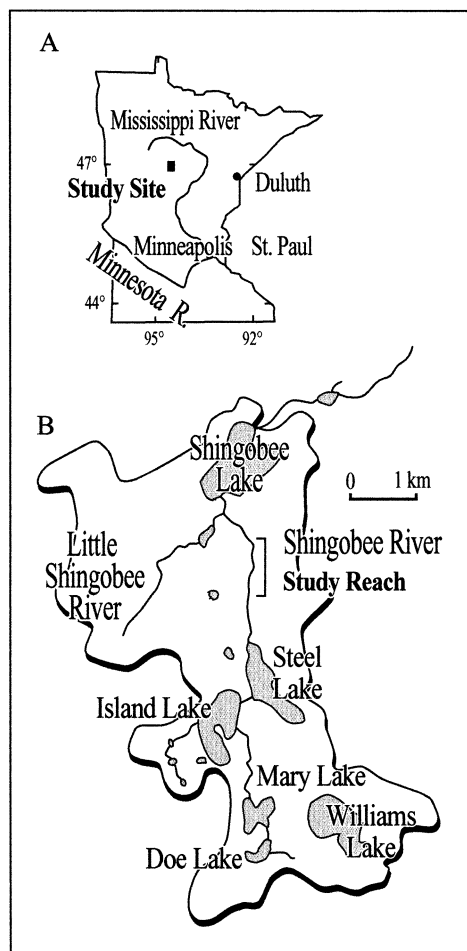


Fig. 1. (A) Minnesota state map. (B) Shingobee River Headwaters Area and the study reach.

cept has fostered an understanding of how groundwater and stream water interact (Winter et al. 1998), this knowledge is rarely incorporated into laboratory experiments (Hakenkamp et al. 1993). Quantifying hyporheic processes in laboratory experiments requires accurate simulations of subsurface flow (Palmer 1993). In the experiments described herein, we developed a sediment perfusion core technique that simulated hydrologic mixing in the stream bed and were used to identify and quantify inorganic N transformation rates in the hyporheic zone of a small midwestern U.S. river.

Study site

The Shingobee River Headwaters Area drains a recently glaciated landscape in north-central Minnesota (Fig. 1A). The terrain is hummocky, with an incompletely developed drainage network. The catchment contains a diverse connection of lakes, streams, wetlands, and groundwater seeps, which promotes extensive interactions between groundwater and surface water.

The study site (Fig. 1B) was located in a 600-m long, free-flowing reach that connects Steel and Shingobee Lakes. This second-order reach, which carries a mean annual dis-

charge of $0.23 \text{ m}^3 \text{ s}^{-1}$, has no tributaries and is the major hydrologic input to Shingobee Lake. The channel has a relatively uniform width (3–4 m) and depth (20 cm), with a low gradient (0.004) (Duff et al. 1999).

The Shingobee River is a groundwater-dominated stream, with groundwater entering as diffuse and focused discharge through the bed and as bank-side seeps. Groundwater discharge has been estimated by chloride dilution experiments, vertical hydraulic gradients, seepage meter measurements, and temperature profiles in the stream bed (Duff et al. 1997; Jackman et al. 1997). In one experiment, Jackman et al. (1997) demonstrated, on the basis of chloride dilution, an increase of 13%, or 24 L s^{-1} , in discharge over the 600-m study reach. Groundwater discharge estimates ranged from 0.005 to $0.62 \text{ L m}^{-2} \text{ s}^{-1}$ for diffuse and focused discharge, respectively (Duff et al. 1999). These estimates of groundwater discharge were determined in the same season during which we conducted our perfusion experiments.

The stream bed is mostly sand, but small to large (<30 cm) cobbles characterize several riffles located along the study reach. The sand bed supports a sparse growth of submergent aquatic macrophytes that consists mainly of *Elodea canadensis* and *Potamogeton* spp.; however, the stream bed was mostly free of macrophytes during our study. We focused on a single site within the study reach, located at 540 m (as measured from the injection site for stream tracer experiments; Jackman et al. 1997). This sandy site is in an upwelling area (vertical hydraulic gradient, +0.18) that is representative of hydrologic and benthic conditions throughout the reach (Duff et al. 1997).

All experiments used sediment cores from the hyporheic zone, which extends ~ 20 cm into the stream bed (Duff et al. 1998). The average bulk density of the core sediments was 1.65 g cm^{-3} , and the porosity was 0.4. The sediment cores consisted of 9% very coarse-grained sands (>1 mm), 81% medium- to coarse-grained sands (0.25–1.0 mm), and 10% fine-grained sands and silts (<0.25 mm). The organic matter of these sediments ranged 0.2%–2.0%.

Methods

Sediment perfusion core design—Cores were collected in clear polycarbonate tubes that were 22 cm long and 4.92 cm in diameter, with a wall thickness of 0.16 cm (Fig. 2). Holes were drilled at 2-cm intervals lengthwise and sealed with silicone adhesive, to provide access via syringe needles for sampling pore water. One end of each tube was beveled, for easier insertion into the stream bed. Once inserted to the desired depth, the top was capped with a rubber stopper (10½). The sediment core was extracted by gentle vertical pulling and then capped on the bottom. The overlying water was decanted and the core recapped. Three cores, 15–18 cm long, were collected for each experiment. Special care was taken to maintain cores upright and to minimize disturbance during transport. The lag time between collection and the initiation of experiments was 3–4 h.

Groundwater was collected from a minipiezometer at a site of upwelling using a peristaltic field pump (GeoPump) and filtered through $0.22\text{-}\mu\text{m}$ filters into a multilayered gas-

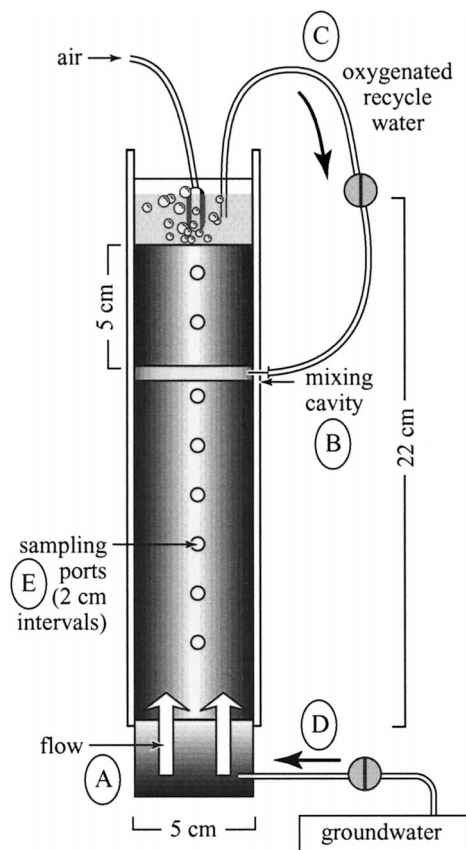


Fig. 2. Diagram of the perfusion core setup. (A) The inlet cup provides an even cross-sectional distribution of (D) groundwater into the columns. Flow is initiated upward through the columns. (B) The mixing cavity is installed to provide an even distribution of the (C) aerated recycled water, which is introduced into the columns using a peristaltic pump. (E) Samples were taken from the inlet, outlet, and sampling ports along the length of the column.

sampling bag (Alltech; P/N 4192). The gas-sampling bags minimized atmospheric exchange and kept the groundwater from oxygenating during the experiment. This water was low in NO_3^- ($\leq 5 \mu\text{g N L}^{-1}$) and high in ammonium (NH_4^+) ($\sim 300 \mu\text{g N L}^{-1}$), as is characteristic of groundwater discharge throughout the reach.

In the laboratory, the bottom cap was removed and an inlet reservoir installed. The column inlet reservoir ensured even cross-sectional distribution of the groundwater perfused into each core. Each inlet reservoir was a 60-ml plastic container (Fig. 2A). A piece of fine-mesh Nitex screen, placed on top of the inlet container, prevented sediment from falling into the reservoir. Containers were filled with groundwater, attached to the bottom of each core, and sealed with several layers of parafilm.

A recycle loop at the top of each core simulated surface-water penetration into bed sediments (Fig. 2C). The overlying water in each core varied 2–4 cm in depth and was aerated using an aquarium air pump and air stones. Overlying water was pumped back into a mixing cavity at a depth of ~ 5 cm. To install the mixing cavity (Fig. 2B), the upper sediment was removed from the cores in 1-cm intervals, the

mixing cavity was then placed into the core, and the sediment was repacked to approximately retain natural stratification with 1-cm resolution. The actual placement of the mixing cavity was based on color differences between the oxic brown and reduced gray-black sediment that effectively distinguished these two conditions (Patrick and Reddy 1976; Nishio et al. 1982). The mixing zone, which simulated the actual depth of surface water penetration, was 5–6 cm. The mixing cavity helped provide a one-dimensional flow system that simplified subsequent modeling (Sheibley et al. in press).

Once the cores were assembled, water was pumped with a peristaltic pump from the closed groundwater bag into each column, initiating upward flow, to simulate groundwater discharge (Fig. 2D). At the mixing cavity, aerated surface water mixed with the perfusing groundwater, mimicking in situ groundwater–surface water interactions. For each experiment, a multichannel peristaltic pump (Masterflex; 7519-25) ran three cores simultaneously. The inlet flow rate was $1.0 \pm 0.1 \text{ ml min}^{-1}$, simulating vertical fluxes typical of upwelling areas in the channel (Jackman et al. 1997; Duff et al. 1999). The recycle loop flow rate was $3.9 \pm 0.4 \text{ ml min}^{-1}$, which maintained a highly oxygenated surface sediment zone. A typical perfusion core experiment ran 5–7 d.

Perfusion core experiments—The perfusion core experiments were conducted in September 1998 at room temperature (22°C). At this time, Shingobee River stream water temperature was $\sim 18^\circ\text{C}$. Additional perfusion core experiments investigating the effect of temperature and season on nitrogen cycling in the hyporheic zone are presented in Sheibley et al. (in press).

The gas-sampling bags used for the groundwater reservoirs were equipped with gas-tight septa, allowing liquid and gas amendment to the groundwater. In all experiments, dissolved oxygen (O_2) was maintained at in situ levels ($\text{O}_2 < 1.0 \text{ mg L}^{-1}$) by sparging the groundwater with N_2 before the beginning of the experiments. The groundwater remained anoxic throughout the experiments. Additional amendments to the groundwater included bromide (Br^-), acetylene (C_2H_2), and NO_3^- on an experiment-specific basis, as described later and summarized in Table 1.

Br^- breakthrough experiment— Br^- was added to the inlet groundwater of four cores. The four columns were perfused with Br^- -spiked groundwater with an average flow rate of $0.86 \pm 0.08 \text{ ml min}^{-1}$. One milliliter of water was collected from the outlet of the columns with a syringe and filtered ($0.45 \mu\text{m}$) into plastic test tubes at regular intervals. Br^- breakthrough curves estimated the groundwater travel time through the column and the onset of hydrologic steady state and served as a conservative tracer for inorganic N transformations. Tracer experiments were run for 10 h, ~ 4 –5 hydraulic residence times.

Ambient dissolved inorganic nitrogen (DIN) perfusion—Perfusion experiments using water with ambient levels of NH_4^+ and NO_3^- were conducted to identify N cycling processes and rates. Water samples were collected for NO_3^- , nitrite (NO_2^-), and NH_4^+ at the inlet and outlet of each col-

Table 1. Experimental conditions during three perfusion experiments, September 1998.

Experiment	No. of cores	Date	Groundwater treatment
Bromide breakthrough	4	10	N ₂ ,* spiked with Br ⁻ (1 mg L ⁻¹ , final concentration)
Ambient DIN perfusion	3	3–9	Na ₂ ,* added C ₂ H ₂ † at 130 h
Denitrification potentials	4	19–24	N ₂ ,* C ₂ H ₂ ,† added 150 μg N L ⁻¹ NO ₃ ⁻ at 24 h, 1,500 μg N L ⁻¹ NO ₃ ⁻ at 72 h (final concentration)
Exchangeable NH ₄ ⁺	6	3–11	N ₂ ,* KCl extractions before and after perfusion

* Sparged groundwater for 1 h.

† Sparged groundwater for 1–2 min.

umn. In addition, depth profiles of DIN were collected from sampling ports distributed along the length of the columns (Fig. 2E). Pore water was withdrawn with a 20-gauge needle and peristaltic pump at a rate of 0.34 ± 0.04 ml min⁻¹, to preserve natural pore water gradients. Approximately 24 ml of pore water was withdrawn (4 ml per sample at six depths) for each profile over 2 h. Instantaneous water volume in each core was ~230 ml. All water samples were filtered through a 0.45-μm syringe filter into disposable plastic containers and frozen until analysis. After 130 h of perfusion, the groundwater was sparged with C₂H₂ for 1 min, and perfusion was continued, to examine its effect on the concentrations of NH₄⁺ and NO₃⁻ at the outlet. Acetylene inhibits NH₄⁺ oxidation (nitrification) by blocking ammonia mono-oxygenase enzymes in nitrifying bacteria (Hynes and Knowles 1978).

Denitrification potential—The C₂H₂ block technique was used to estimate the denitrification potential (Yoshinari and Knowles 1976). Groundwater was sparged with C₂H₂ for 2 min, and either 150 or 1,500 μg N L⁻¹ (final concentration) as KNO₃ was added to the groundwater reservoir to increase background NO₃⁻ concentrations high enough to quantify the N₂O accumulation. Both NO₃⁻ and N₂O were measured in the inlet, outlet, and pore water. Nitrous oxide samples were collected from the inlet, outlet, and pore water by withdrawing a water sample into a 1-cm³ plastic syringe with a 22-gauge needle. Samples were taken slowly by hand then transferred into 2- or 3-ml sample vials equipped with airtight septa. The sample vials were preflushed with N₂O-free N₂ for several minutes, to eliminate atmospheric N₂O. Samples were stored upside down and equilibrated for several hours before the analysis of headspace gas for N₂O.

Exchangeable NH₄⁺ in sediment perfusion cores—Exchangeable NH₄⁺ was measured in sediment perfusion experiments to determine whether groundwater perfusion resulted in significant NH₄⁺ sorption onto sediments. Six cores were collected, of which two were processed immediately

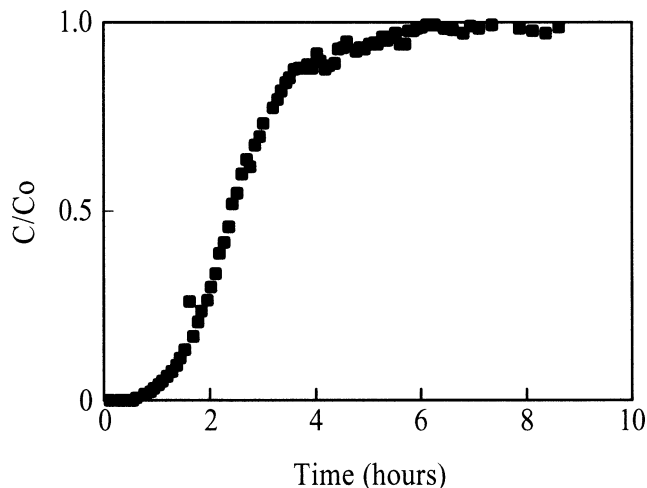


Fig. 3. Br⁻ breakthrough curve, September 1998. Data points are the average of four columns. C/Co, the Br⁻ concentration in the outlet divided by the Br⁻ concentration in the inlet. The nominal travel time is the time to reach one-half the plateau value (C/Co = 0.5), which was ~2.25 h. Hydrologic steady state was reached within 6 h.

and the remaining four at the end of an ambient DIN perfusion. Sediment cores were extruded in 3-cm-long sections: 0–3, 3–6, 6–9, 9–12, and 12–15 cm. Exchangeable NH₄⁺ was determined with 10-ml sediment aliquots extracted with 100 ml of 2 mol L⁻¹ KCl for 1 h (Keeney and Nelson 1982). The supernatant liquid was filtered through 0.45-μm syringe filters and analyzed for NH₄⁺-N.

Analytical procedures—Ammonium-nitrogen (NH₄⁺-N) was determined using the salicylate-hypochlorite spectrophotometric method (Bower and Holm-Hansen 1980). Nitrate, NO₂⁻, and Br⁻ were determined on an ion chromatograph (Dionex DX 500) equipped with an autosampler and a 100-μl sample loop. The system had an AS4A-SC (4 mm) analytical column and an AG4A-SC (4 mm) guard column. The eluent was a 1.8/1.7 mmol L⁻¹ sodium carbonate/bicarbonate solution (flow rate, 2.00 ml min⁻¹). Minimum detection limits were 10 and 3 μg N L⁻¹ for NH₄⁺ and NO₃⁻, respectively. Nitrous oxide was analyzed on a ⁶³Ni electron-capture detector gas chromatograph (Shimadzu Scientific Instruments) with a Poropak R column. The oven and detector temperatures were 60°C and 300°C, respectively. A column-switching valve separated N₂O from C₂H₂ (Duff et al. 1996). The carrier gas was a mixture of methane (5%) and argon (95%) at a flow rate of 30 ml min⁻¹. The quantity of N₂O in the original water sample was calculated using the Bunsen solubility coefficient (Weiss and Price 1980). Nitrous oxide analyses were done within 5 h of collection.

Results

Br⁻ breakthrough curves—When Br⁻ (the conservative tracer) was introduced via groundwater input into four columns, Br⁻ reached a plateau concentration in the outlet after 6 h and remained constant until the experiment was terminated (Fig. 3). At the plateau concentration, the Br⁻ concen-

tration in the outlet was 100% of the inlet. The nominal travel time—the time until Br^- concentration reached one-half the plateau value—through the columns was 2.25 h. The breakthrough curve was similar in columns without a recycle loop (data not shown), which indicates that travel times were not significantly altered by the mixing cavity and recycle loop.

Ambient DIN perfusion—During the first day of every experiment, water exiting the columns contained NH_4^+ and NO_3^- at concentrations above the ambient level, with NH_4^+ peaking first. At peak flush, NH_4^+ and NO_3^- levels in the outlet were ~ 400 and $225 \mu\text{g N L}^{-1}$ higher than in the groundwater inlet, respectively. After the flush, groundwater NH_4^+ typically decreased during perfusion of water through the columns, declining from $300 \mu\text{g N L}^{-1}$ at the inlet to $50 \mu\text{g N L}^{-1}$ in the outlet (Fig. 4A). Conversely, NO_3^- increased from $\sim 5 \mu\text{g N L}^{-1}$ in the inlet to $\sim 50 \mu\text{g N L}^{-1}$ in the outlet (Fig. 4B). After the addition of C_2H_2 to the groundwater reservoir at 130 h, NH_4^+ and NO_3^- slowly increased in the direction of inlet concentrations (Fig. 4C).

Depth profiles at steady state indicated statistically uniform NH_4^+ and NO_3^- concentrations in the low- O_2 sediment below the recycle loop (Fig. 5A; $P < 0.05$, one-way analysis of variance [ANOVA]). However, there was nearly complete removal of NH_4^+ in the upper region and a concomitant increase in NO_3^- , averaging $\sim 25\%$ of the NH_4^+ decrease, which was presumably supported by the aerated recycled water (entering at the dashed line, Fig. 5A). When the aerated recycled water was absent from the columns in the presence of C_2H_2 , depth profiles for NH_4^+ and NO_3^- became statistically uniform throughout the column (Fig. 5B; $P < 0.05$, one-way ANOVA).

Nitrification was estimated from NH_4^+ loss and NO_3^- formation between the inlet, outlet, and pore water of the cores. Ammonium loss and NO_3^- formation rates were calculated per cm^3 sediment (including the interstitial water volume) using the following equations:

$$r_1 = \frac{(\Delta\text{NH}_4^+) \cdot Q}{V} \quad (1)$$

$$r_2 = \frac{(\Delta\text{NO}_3^-) \cdot Q}{V} \quad (2)$$

where Δ is change in concentration of NH_4^+ or NO_3^- ($\mu\text{g N L}^{-1}$), Q is the volumetric flow rate (L min^{-1}), and V is the sediment volume (cm^3) in the zone responsible for the DIN changes (sediment plus water), not the total column volume. Nitrate reduction rates were estimated from the difference between the NH_4^+ disappearance and NO_3^- formation rates using the following equation:

$$r_3 = r_1 - r_2 \quad (3)$$

where r_3 is the NO_3^- reduction rate and r_1 and r_2 are defined above.

Rates of NH_4^+ loss, NO_3^- formation, and NO_3^- reduction from Eqs. 1, 2, and 3 are shown in Table 2. The NH_4^+ loss rates for the three columns ranged 1.76 – $2.99 \mu\text{g N cm}^{-3} \text{ d}^{-1}$. Nitrate formation rates from cores ranged 0.42 – $0.82 \mu\text{g N}$

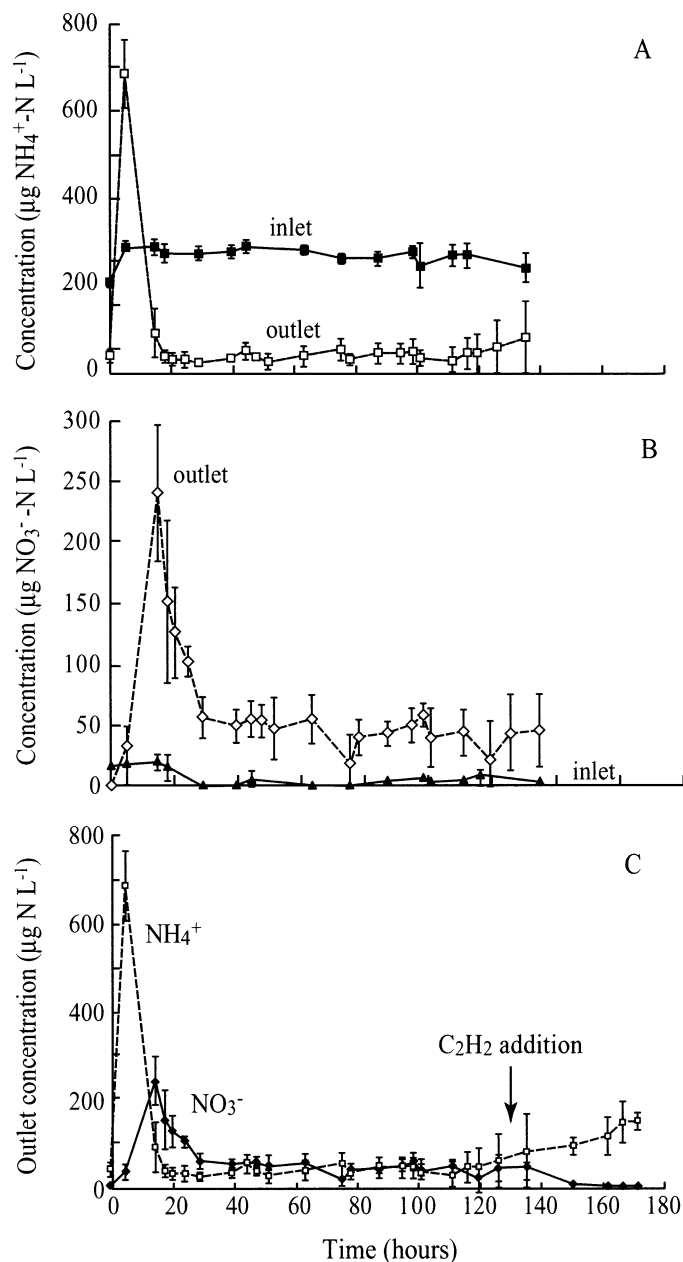
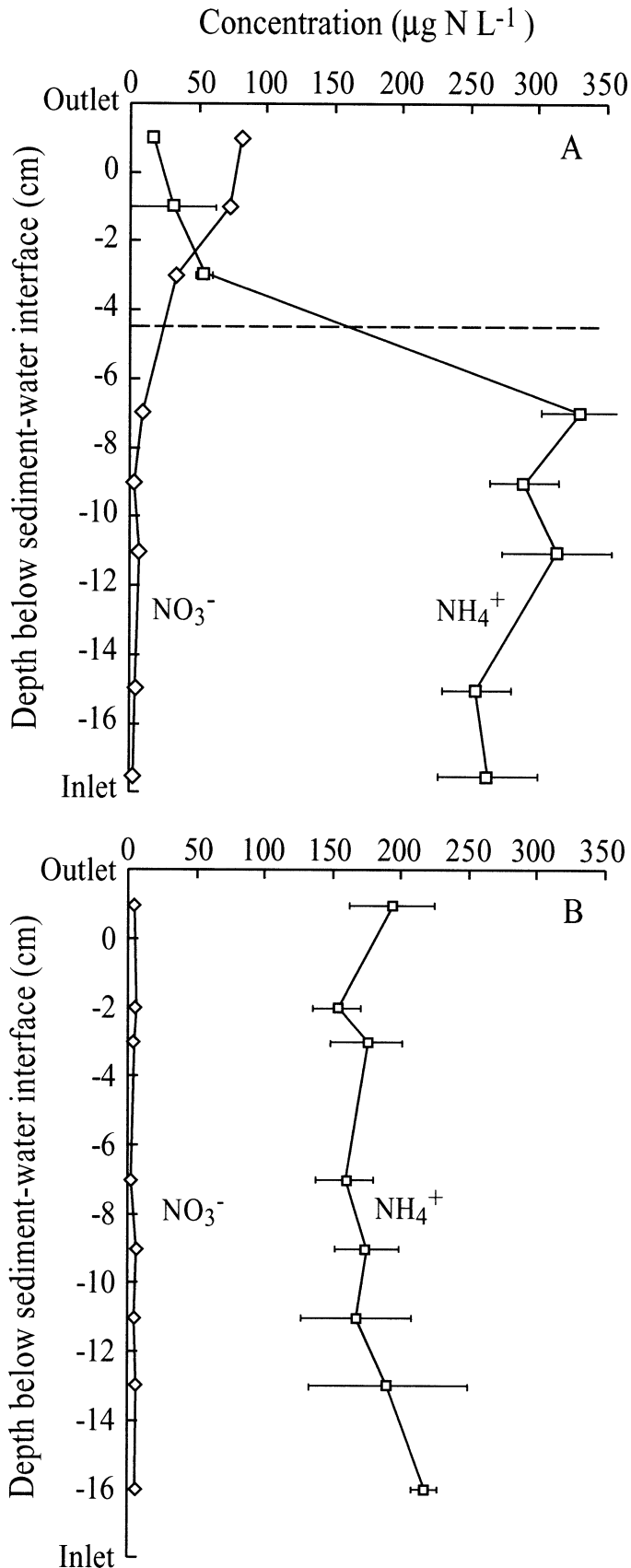


Fig. 4. Plot of inlet and outlet concentration for (A) NH_4^+ and (B) NO_3^- during one ambient DIN perfusion experiment, September 1998. (C) Outlet NH_4^+ and NO_3^- concentration after the addition of C_2H_2 at 130 h. Data in all plots represent average concentrations (\pm SD) from three columns.

$\text{cm}^{-3} \text{ d}^{-1}$. By difference, rates of NO_3^- reduction ranged 0.98 – $2.28 \mu\text{g N cm}^{-3} \text{ d}^{-1}$ ($\bar{x} = 1.53 \pm 0.67 \mu\text{g N cm}^{-3} \text{ d}^{-1}$).

Denitrification potential—In our experiment, the nitrate concentration was sequentially elevated in the groundwater reservoir from ambient to 150 to $1,500 \mu\text{g N L}^{-1}$ over 160 h of perfusion. During the entire experiment, the level of effluent NO_3^- was negligible (Fig. 6), indicating complete loss during perfusion. At $150 \mu\text{g NO}_3^- \text{ N L}^{-1}$, all NO_3^- disappeared within 2–3 cm of the inlet (Fig. 7A). At $1,500 \mu\text{g}$



NO_3^- -N L^{-1} , complete removal occurred within 6–7 cm (Fig. 7B). Nitrous oxide accumulated at both levels in the presence of C_2H_2 . The N_2O production accounted for $\sim 58\%$ of the observed NO_3^- loss in the low amendment column and nearly 100% of the NO_3^- loss in the high amendment column (on a gram-to-gram N basis). Nitrous oxide decreased in the upper column because of degassing during aeration of the overlying water and the recycling of that water through the upper column.

Nitrate reduction rates were calculated from the NO_3^- loss, and the denitrification potential was calculated from N_2O accumulation in column pore water (Table 3). Nitrate reduction rates and denitrification potentials were calculated similar to Eqs. 1 and 2 by substituting ΔNO_3^- and $\Delta\text{N}_2\text{O}$ for ΔNH_4^+ and ΔNO_3^- , respectively. The sediment volume used to calculate NO_3^- reduction rates and denitrification potentials was limited to the zone responsible for the observed change in NO_3^- or N_2O , as indicated by concentration profiles. At an inlet concentration of $150 \mu\text{g NO}_3^- \text{N L}^{-1}$, NO_3^- reduction rates (as NO_3^- removed) ranged 1.24 – $5.15 \mu\text{g N cm}^{-3} \text{ d}^{-1}$, with an average of $3.44 \pm 1.66 \mu\text{g N cm}^{-3} \text{ d}^{-1}$. At $1,500 \mu\text{g NO}_3^- \text{N L}^{-1}$, the NO_3^- reduction rates were ~ 4 times greater, ranging 10.89 – $16.60 \mu\text{g N cm}^{-3} \text{ d}^{-1}$ ($\bar{x} = 14.25 \pm 2.44 \mu\text{g N cm}^{-3} \text{ d}^{-1}$). Similarly, mean denitrification potential (as N_2O -N produced) increased from 1.46 ± 0.76 to $12.19 \pm 2.51 \mu\text{g N cm}^{-3} \text{ d}^{-1}$ for the 150 and $1,500 \mu\text{g NO}_3^- \text{N L}^{-1}$ additions, respectively.

Exchangeable NH_4^+ in sediment perfusion cores—Exchangeable NH_4^+ ranged 1.1 – 2.0 and 1.3 – $2.3 \mu\text{g NH}_4^+ \text{N g sediment}^{-1}$ respectively, for cores extracted immediately and after several days of perfusion (Fig. 8). No statistically significant increases in extractable NH_4^+ were observed in cores before and after multiday perfusions at any depth ($P < 0.05$, one-way ANOVA), which indicates that NH_4^+ depletion during perfusion did not result from sorption.

Discussion

Streambed sediments are biogeochemically active zones where advective transport can influence nutrient cycling (Grimm and Fisher 1984; Hendricks 1993; Duff and Triska 2000). Sediment perfusion cores with a recycle loop simulate the stream bed's hydrologic and biological interactions, allowing estimates of nutrient cycling under quasi in situ conditions. Perfusion cores have several advantages over traditional flask assays for determining in situ N cycling rates. Unlike slurry in a flask, sediment cores are relatively undisturbed and therefore maintain natural chemical gradients and

←

Fig. 5. (A) Depth profile for NH_4^+ and NO_3^- during an ambient DIN perfusion experiment, September 1998. Aerated recycled water was introduced into the column at 4.5-cm depth (dashed line). Data represent an average concentration (± 1 SD) in one column over 3 d during steady state before the introduction of C_2H_2 to the groundwater. (B) Depth profile for NH_4^+ and NO_3^- during a perfusion experiment with C_2H_2 added and the recycle removed, September 1998.

Table 2. NH_4^+ loss rates, NO_3^- formation rates, and NO_3^- reduction rates based on NH_4^+ and NO_3^- concentration gradients in perfusion cores in September 1998. Rates are presented on a cm^3 sediment basis (which includes interstitial water). Nitrate reduction rates are determined by the difference between the NH_4^+ loss and NO_3^- production rates. Average rates are ± 1 SD ($n = 3$).

Column	NH_4^+ loss rate ($\mu\text{g N cm}^{-3} \text{ d}^{-1}$)	NO_3^- formation rate ($\mu\text{g N cm}^{-3} \text{ d}^{-1}$)	NO_3^- reduction rate ($\mu\text{g N cm}^{-3} \text{ d}^{-1}$)
1	1.80	0.82	0.98
2	1.76	0.42	1.34
3	2.99	0.71	2.28
Average	2.18 ± 0.70	0.65 ± 0.20	1.53 ± 0.67

biomass distribution. In addition, they simulate hydrologic characteristics such as diffusion, dispersion, and advection, which influence biogeochemical process rates.

Studies of N transformations in stream sediments that have used perfusion cores are rare. Sain et al. (1977), who examined NO_3^- loss in water overlying stream sediments, found that NO_3^- loss increased with increasing temperature. Stammers et al. (1983), who examined denitrification in stream sediment cores where NO_3^- diffused from overlying water into columns, demonstrated zero-order kinetics for NO_3^- loss, indicating that rates were independent of concentration. Core studies that have incorporated a flow component include those of Fiebig (1992), who examined the fate of dissolved organic N (as amino acids), and Fiebig and Lock (1991). Both found that a large fraction of groundwater-derived dissolved organic carbon (DOC) and associated N was immobilized in the stream bed, a potential energy and nutrient source for stream organisms. Finally, Blicher-Mathiesen and Hoffmann (1999) used perfusion cores to demonstrate denitrification of NO_3^- -rich, agriculturally impacted groundwater during discharge through organic-rich soils of a riparian fen.

In Shingobee River perfusion cores, DIN steady state was

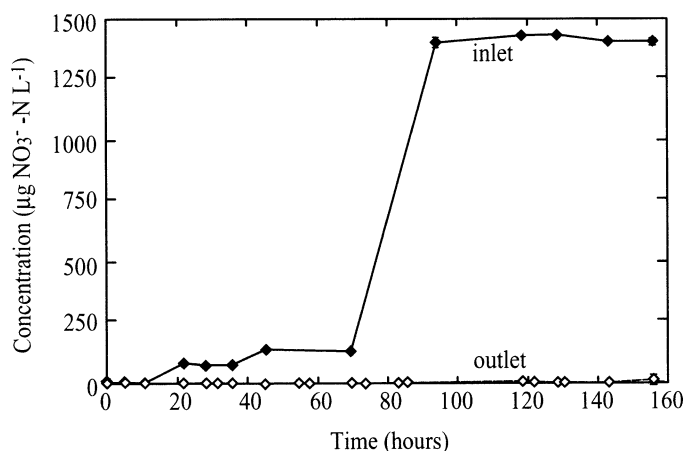


Fig. 6. Inlet and outlet NO_3^- concentrations during a denitrification potential experiment, September 1998. Inlet groundwater was amended with $150 \mu\text{g NO}_3^- \text{ N L}^{-1}$ after day 1 and then raised to $1,500 \mu\text{g NO}_3^- \text{ N L}^{-1}$ after day 3. Data represent averages (\pm SD) from four columns.

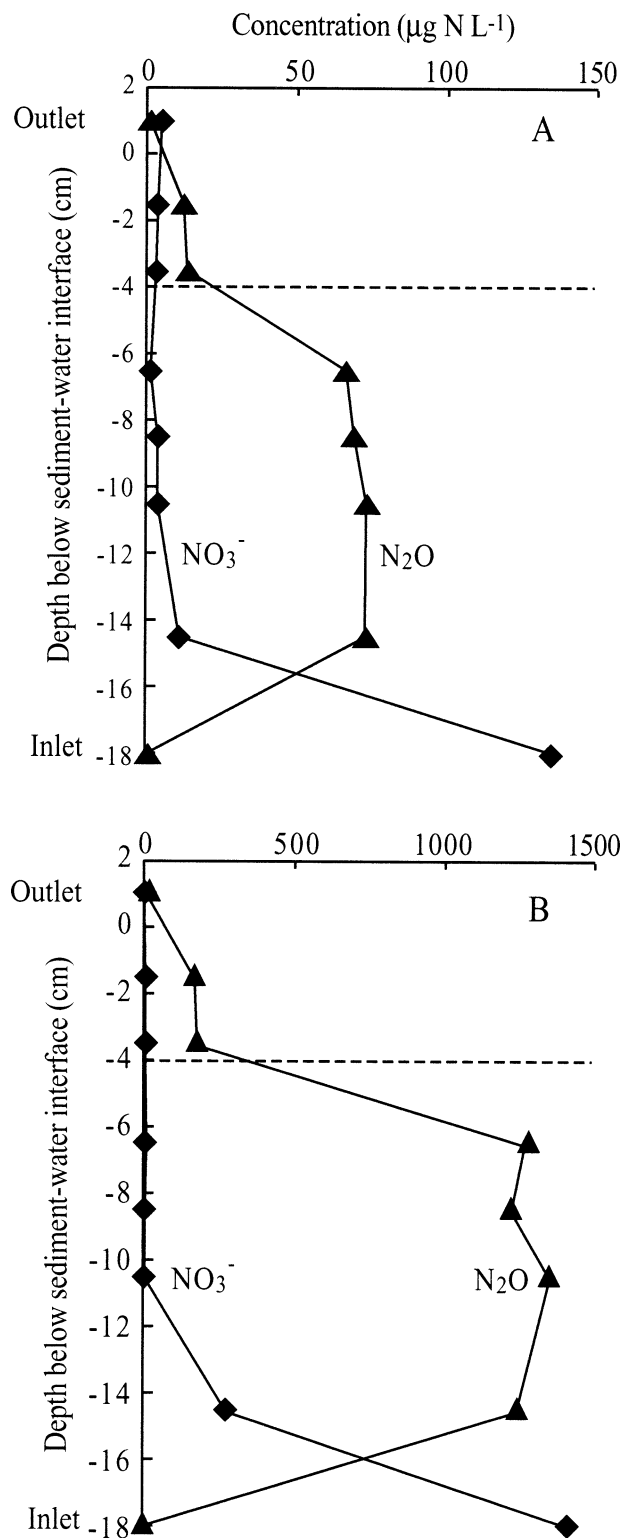


Fig. 7. Depth profile for NO_3^- and N_2O 24 h after C_2H_2 and (A) $150 \mu\text{g NO}_3^- \text{ N L}^{-1}$ and (B) $1,500 \mu\text{g NO}_3^- \text{ N L}^{-1}$ were added to the groundwater reservoir, September 1998. Note: scales on the x-axis are different.

Table 3. NO_3^- reduction and N_2O production rates, based on NO_3^- and N_2O concentration gradients in perfusion cores amended with NO_3^- and C_2H_2 in September 1998. Rates are presented on a per cm^3 of sediment basis (including interstitial water). Average rates are ± 1 SD ($n = 4$).

Column	NO_3^- reduction rates ($\mu\text{g N cm}^{-3} \text{d}^{-1}$)	NO_3^- production rates ($\mu\text{g N cm}^{-3} \text{d}^{-1}$)
150 $\mu\text{g NO}_3^- \text{-N L}^{-1}$		
1	4.12	1.25
2	3.26	1.88
3	5.15	2.23
4	1.24	0.49
Average	3.44 ± 1.66	1.46 ± 0.76
1,500 $\mu\text{g NO}_3^- \text{-N L}^{-1}$		
1	15.29	10.89
2	14.23	13.65
3	16.60	14.86
4	10.89	9.36
Average	14.25 ± 2.44	12.19 ± 2.51

approximated within 24 h in all experiments after the initial flush of NH_4^+ and NO_3^- . In contrast, Br^- steady state during the breakthrough experiments was established within 6 h. An initial nutrient flush is common in cores and is often attributed to leaching endogenous substrates (Doner et al. 1974; Hynes and Knowles 1980; Fiebig 1992; Marxsen and Fiebig 1993). In the Shingobee River, removing cores from the natural chemical and hydrologic equilibrium for as little as 4 h presumably resulted in the accumulation and release of NH_4^+ via mineralization. The subsequent NO_3^- pulse was most likely due to the nitrification of mineralized NH_4^+ (Fig. 4A,B). The absence of a Br^- flush during breakthrough experiments indicates that the NH_4^+ and NO_3^- flushes were not a hydrologic artifact of the core protocols. Once approaching steady state, inlet and outlet DIN levels closely simulated DIN levels in groundwater discharge and surface water from the Shingobee River.

Surficial sediments of lakes (Rysgaard et al. 1994), streams (Jones et al. 1995; Mulholland et al. 1997), estuaries (Nishio et al. 1982; Jenkins and Kemp 1984), and oceans (Sorensen 1978b) all exhibit high biological activity. They are also the zones of highest advection and diffusion of substrates. Two redox zones present in aquatic sediments were replicated in the perfusion cores. Below the recycle loop, O_2 was absent and NH_4^+ and NO_3^- profiles were uniform similar to pore water in the Shingobee River (Duff et al. 1998). Above the recycling zone, the introduction of O_2 promoted relatively steep DIN gradients. High transformation rates at this interface signify the importance of surface-water advection for stimulating N transformation during groundwater discharge.

Ammonium decreased in the upper, aerated region of the sediment cores because of (1) volatilization, (2) sorption, (3) assimilative uptake, or (4) nitrification. Although significant NH_3 volatilization occurs at $\text{pH} > 9.0$ (Emerson et al. 1975), the highest recorded pH in Shingobee River surface water was ~ 8 . Groundwater pH typically ranged 7–7.5 (data not

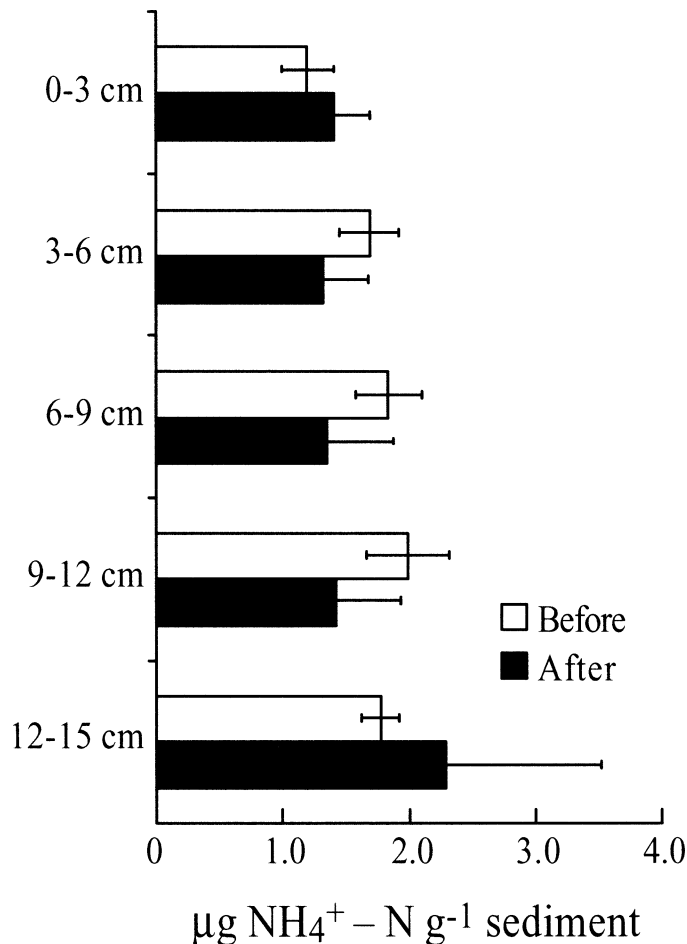


Fig. 8. Exchangeable NH_4^+ before ($n = 9$) and after ($n = 24$) a multiday perfusion experiment, September 1998. Data represent means ± 1 SD. There was no significant difference in exchangeable NH_4^+ before and after perfusion ($P < 0.05$, one-way ANOVA).

shown), which lessens the probability of significant volatilization. Negligible amounts of exchangeable NH_4^+ before and after a 7-d perfusion experiment minimized sorption as a cause of NH_4^+ loss. Uptake associated with photosynthesis also was likely insignificant, because there were no visible plants, roots, or algae observed in the upper sediments. In oligotrophic streams similar to the Shingobee River, periphyton uptake often produces diurnal DIN fluctuation during the summer (e.g., Triska et al. 1989), a pattern not observed in either the perfusion cores or the stream. Therefore, nitrification was the most likely explanation for NH_4^+ loss in the upper sediment.

The NH_4^+ and NO_3^- mass balance between the inlet and outlet reservoirs indicated that $\sim 25\%$ of the entering NH_4^+ was exported as NO_3^- . The addition of C_2H_2 inhibited NH_4^+ oxidation, presumably by inactivating the mono-oxygenase enzyme of the nitrifying bacteria (Hyman and Wood 1985). As a result, NO_3^- disappeared from the column effluent and NH_4^+ approached groundwater levels. A comparable pattern in soil columns led Hynes and Knowles (1980) and Jensen et al. (1993) to suggest that such NO_3^- was produced solely from nitrification. In our experiments, most DIN transfor-

mation occurred over a 4-cm-long transport distance, which indicates that even a thin aerobic interface can effectively process high concentrations of groundwater DIN.

Nitrate exported to the overlying water did not account for the total NH_4^+ loss. If we assume that most NH_4^+ loss was due to nitrification, then significant NO_3^- loss occurred from (1) assimilation, (2) dissimilatory reduction to NH_4^+ , or (3) denitrification. Denitrification is the most likely mechanism, because the assimilatory reduction of NO_3^- to NH_4^+ (ARNA) by microorganisms is inhibited at NH_4^+ concentrations lower than was found in our cores. For example, NH_4^+ concentrations of 80 to as low as $0.5 \mu\text{g N L}^{-1}$ have been reported to suppress NO_3^- assimilation in soil slurries (Rice and Tiedje 1989) and phytoplankton (McCarthy et al. 1977), respectively. Given the high NH_4^+ levels in our experiments ($\sim 300 \mu\text{g NH}_4^+\text{-N L}^{-1}$), the absence of primary producers and lack of change in microbial biomass (phospholipid bioassay, Sheibley unpubl. data), ARNA was likely minimal. Denitrification was also more likely than dissimilatory NO_3^- reduction (DNRA). DNRA tends to predominate in long-term anoxic environments such as deep sediments (Keeney et al. 1971; Sorensen 1978a; Tiedje et al. 1981; Kelso et al. 1997), whereas denitrification is favored in sediment where O_2 is low and fluctuating and redox conditions are less reducing, as is typical of surface sediments (Tiedje et al. 1981; Kelso et al. 1997). Although these two processes may not be spatially well defined in sediment environments, the artificially aerated upper sediments would generally favor denitrification over DNRA. The absence of a 1:1 ratio for NH_4^+ conversion to NO_3^- suggests that a nitrate-reducing population was present and poised to reduce NO_3^- at rates similar to or exceeding its formation.

When NO_3^- was added to the groundwater reservoir, a high denitrification capacity was observed in the first 2–3 cm of the groundwater flow path. High observed rates were presumably sustained by microorganisms using organic material in the stream bed. This rapid disappearance of NO_3^- suggests excess electron donor availability throughout the core. These conclusions are similar to those in soil core perfusions by Blicher-Mathiesen and Hoffmann (1999), who used the organic-rich soils of a riparian fen.

Because we could not directly measure denitrification in the upper sediment, we compared the NO_3^- reduction rates (Table 2) estimated from the DIN mass balances with denitrification potentials estimated from N_2O profiles in the lower sediment (Table 3). Nitrate concentrations ranged 1–150 $\mu\text{g NO}_3^-\text{-N L}^{-1}$ in the Shingobee River (data not shown), reaching maxima similar to the NO_3^- levels used in the first denitrification potential assay (150 $\mu\text{g NO}_3^-\text{-N L}^{-1}$). At ambient DIN levels in the cores, the calculated NO_3^- reduction (denitrification) rates ranged 0.98–2.28 $\mu\text{g N cm}^{-3} \text{d}^{-1}$, compared with 0.49–2.23 $\mu\text{g N cm}^{-3} \text{d}^{-1}$ during the denitrification potential assays. The similarity between the denitrification potential estimates suggests that the NO_3^- reduction rates calculated by difference in the upper sediments are reasonable estimates.

Nitrous oxide evolution accounted for 58% to $\sim 100\%$ of the NO_3^- lost during the C_2H_2 inhibition assays. Lower conversion rates may result from incomplete inhibition of N_2O reductase, which has been observed at low NO_3^- concentra-

Table 4. Comparison of nitrification rates from the literature and the present study.

Type of sediment	Nitrification rate ($\text{mg N m}^{-2} \text{d}^{-1}$)	Reference
Lake	30	DeLaune and Smith (1987)
Estuary	3–112	Binnerup et al. (1992)
Marine	840	Sloth et al. (1992)
Lake	125	Jensen et al. (1993)
Lake	50–68	Rysgaard et al. (1994)
Lake	74	Jensen et al. (1994)
Stream	84	Jones et al. (1995)
Stream	42–209*	Present study
	$\mu\text{g N cm}^{-3} \text{d}^{-1}$	
Stream	0–2.5	Triska et al. (1993a)
Stream	0–1.2	Strauss and Lamberti (2000)
Stream	0.42–2.99	Present study

* Rates were converted from $\mu\text{g N cm}^{-3} \text{d}^{-1}$ to $\text{mg N m}^{-2} \text{d}^{-1}$ using the ratio of sediment volume to cross-sectional area.

tions in stream (Christensen et al. 1989) and estuarine (Kaspar 1982) sediments. Denitrification, which is commonly observed in surface sediments of streams, lakes, coastal, and estuarine sediments, can occur in anaerobic microsites within an otherwise aerobic environment. Soils and sediments are highly heterogeneous, and aggregates containing an aerobic surface and an anaerobic center are common (Killham 1994; Kemp and Dodds 2002). Misra et al. (1974), using soil columns, found nitrification on the exterior of soil aggregates and denitrification within. Hynes and Knowles (1980) assumed nitrification-denitrification coupling at near-atmospheric concentrations of O_2 surrounding water-saturated soil aggregates. Jenkins and Kemp (1984) also observed nitrification-denitrification coupling in the upper zone of estuarine sediments. In streams, Hendricks (1993) described the hyporheic zone at Maple River, Michigan, as a patchy environment in which nitrification, denitrification, and ammonification occurred simultaneously. Finally, Duff and Triska (1990) injected NO_3^- and C_2H_2 dissolved in stream water into a subsurface flow path at Little Lost Man Creek, California, and demonstrated that indigenous bacterial populations were capable of transforming NO_3^- to N_2O in anaerobic microsites under oxic background conditions. Therefore, there is ample evidence that nitrification and denitrification, which require distinctly different redox conditions, commonly co-occur in close proximity in soils and sediments (McLaren 1970; DeLaune and Smith 1987).

Nitrification rates ranged from 0.42 $\mu\text{g N cm}^{-3} \text{d}^{-1}$ (as NO_3^- formed, Table 2) to 2.99 $\mu\text{g N cm}^{-3} \text{d}^{-1}$ (as NH_4^+ lost, Table 2). Nitrate reduction rates (denitrification), determined from the difference between the NH_4^+ lost and NO_3^- produced, ranged 0.89–2.28 $\mu\text{g N cm}^{-3} \text{d}^{-1}$. Nitrification and denitrification rates calculated from the DIN mass balance in the core experiments fall within the range of rates reported for lake, coastal, and fluvial sediments (Tables 4 and 5). Nitrification rates reported in the literature range 1–840 $\text{mg N m}^{-2} \text{d}^{-1}$, compared with the 42–209 $\text{mg N m}^{-2} \text{d}^{-1}$ in the present study. Denitrification rates reported in the literature range 4–500 $\text{mg N m}^{-2} \text{d}^{-1}$, with coastal sediments at the

Table 5. Comparison of denitrification rates from the literature and the present study.

Type of sediment	Denitrification rate (mg N m ⁻² d ⁻¹)	Reference
Stream	61–166	Sain et al. (1977)
Lake	100–500	Andersen (1977)
Coastal	14	Sorensen (1978b)
Stream	110	Stammers et al. (1983)
Stream	114–416	Christensen et al. (1989)
Estuary	50–476	Binnerup et al. (1992)
Lake	41	Jensen et al. (1993)
Lake	39–71	Rysgaard et al. (1994)
Lake	54	Jensen et al. (1994)
Coastal	4–7	Nielsen and Guld (1996)
Stream	53–160*	Present study
	$\mu\text{g N cm}^{-3} \text{ d}^{-1}$	
Stream	0–4.7	Triska et al. (1993b)
Stream	0.98–2.28	Present study

* Rates were converted from $\mu\text{g N cm}^{-3} \text{ d}^{-1}$ to $\text{mg N m}^{-2} \text{ d}^{-1}$ using the ratio of sediment volume to cross-sectional area.

lower end of this range. The rates of NO_3^- reduction presented in the present study, 53–160 $\text{mg N m}^{-2} \text{ d}^{-1}$, fell within this range.

Our rates of nitrification and NO_3^- reduction are based on depth profiles in the cores. Because of the small number of sampling ports adjacent to the aerobic-anaerobic interface, our rates may underestimate in situ rates. Ammonium levels do not decrease in the cores until groundwater reaches the mixing cavity. By analogy, most N-cycling activity associated with nitrification-denitrification in the bed of the Shingobee River would be controlled by O_2 advection into shallow surface sediments.

The recycled water in the cores was constantly sparged with air. As a result, upper core sediment was probably more evenly oxygenated than in situ. This condition could produce higher estimated rates of nitrification and lower estimated rates of denitrification than occur in situ. The future development of methods to adequately characterize in situ redox and oxygen gradients in the high-flow stream environment is needed to quantitatively resolve this issue.

All of our perfusion-core experiments were conducted with sediments from one location along the Shingobee River. Although one site cannot represent the total geomorphic, hydrologic, and chemical variability in the study reach, our site was representative of measured diffuse groundwater seepage fluxes within the reach. In a detailed study of groundwater discharge in the study reach, Duff et al. (1999) estimated that “diffuse” groundwater flux across the bed surface accounted for 90% of the groundwater entering the reach, with focused groundwater flux contributing the balance. An estimate of the stream bed areas influenced by focused discharge was only 0.2% of the total reach. Therefore, cores from this single location do represent the hydrologic conditions characteristic of the overall reach.

Patterns of nitrification and NO_3^- reduction calculated from DIN gradients in the sediment perfusion cores can be incorporated into a conceptual model for inorganic N cycling

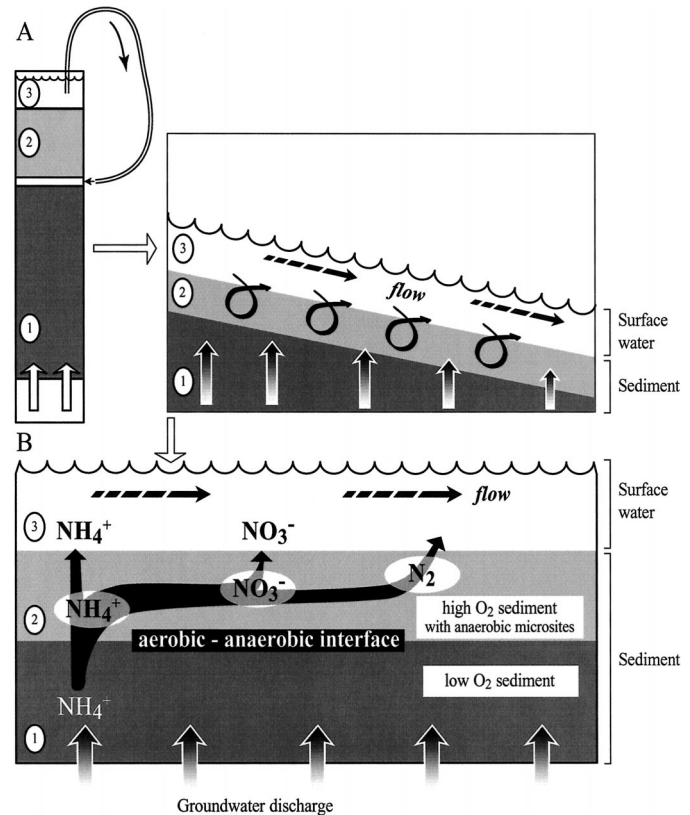


Fig. 9. (A) Comparison between perfusion experiments and the Shingobee River with respect to (1) groundwater discharge, (2) surface water penetration, and (3) the surface stream. (B) Summer-fall conditions for N processing in the hyporheic zone of the Shingobee River. Ammonium-rich groundwater is discharged through the stream bed, passing with little transformation until it reaches the aerobic-anaerobic interface, where NH_4^+ is converted to NO_3^- via nitrification. Most of the NO_3^- formed is quickly reduced via denitrification. A small percentage of both NH_4^+ and NO_3^- is exported to the stream.

in the hyporheic zone of the Shingobee River. The perfusion cores effectively simulated in situ interactions between hydrologic, chemical, and biotic processes occurring within the stream bed (Fig. 9A). An aerobic-anaerobic interface forms where low O_2 groundwater discharged through the stream bed mixes with aerobic stream water exchanged to a shallow depth within the bed (Fig. 9B). Above the mixing interface, NH_4^+ is oxidized to NO_3^- . A small proportion of both NH_4^+ and NO_3^- is exported to the stream, but most NH_4^+ is lost, presumably from coupled nitrification-denitrification. Seasonally, the magnitude of DIN flux out of the sediment is controlled by temperature (Sheibley et al. in press). The relative scale of groundwater discharge to the effective depth of surface water penetration into the bed controls the extent of N transformation as water flows through the Shingobee River.

The results from the present study demonstrate the importance of integrating the hydrology and biology of the hyporheic zone into laboratory experiments. Perfusion cores designed to replicate the hydrologic conditions observed at the Shingobee River allowed us to identify N cycling pro-

cesses and rates. Our results show that groundwater-surface water mixing controlled nitrification-denitrification coupling in the upper sediment.

References

- ANDERSEN, J. M. 1977. Rates of denitrification of undisturbed sediment from six lakes as a function of nitrate concentration, oxygen and temperature. *Arch. Hydrobiol.* **80**: 147-159.
- ARDANKANI, M. S., J. T. REHBOCK, AND A. D. MCLAREN. 1974. Oxidation of ammonium to nitrate in a soil column. *Soil Sci. Soc. Am. Proc.* **38**: 96-99.
- BINNERUP, S. J., K. JENSEN, N. P. REVSBECH, M. K. JENSEN, AND J. SORENSEN. 1992. Denitrification, dissimilatory reduction of nitrate to ammonium, and nitrification in a bioturbated estuarine sediment as measured with ^{15}N and microsensor techniques. *Appl. Environ. Microb.* **58**: 303-313.
- BLICHER-MATHIESEN, G., AND C. C. HOFFMANN. 1999. Denitrification as a sink for dissolved nitrous oxide in a freshwater riparian fen. *J. Environ. Qual.* **28**: 257-262.
- BOWER, C. E., AND T. HOLM-HANSEN. 1980. A Salicylate-Hypochlorite method for determining ammonia in seawater. *Can. J. Fish. Aquat. Sci.* **37**: 794-798.
- CHRISTENSEN, P. B., L. P. NIELSEN, N. P. REVSBECH, AND J. SORENSEN. 1989. Microzonation of denitrification activity in stream sediments as studied with a combined oxygen and nitrous oxide microsensor. *Appl. Environ. Microb.* **55**: 1234-1241.
- DELAUNE, R. D., AND C. J. SMITH. 1987. Simultaneous determination of nitrification and nitrate reduction in sediment-water columns by nitrate-15 dilution. *J. Environ. Qual.* **16**: 227-230.
- DONER, H. E., M. G. VOLZ, AND A. D. MCLAREN. 1974. Column studies of denitrification in soil. *Soil Biol. Biochem.* **6**: 314-346.
- DUFF, J. H., F. MURPHY, C. C. FULLER, F. J. TRISKA, J. W. HARVEY, AND A. P. JACKMAN. 1998. A mini drivepoint sampler for measuring pore water solute concentrations in the hyporheic zone of sand-bottom streams. *Limnol. Oceanogr.* **43**: 1378-1383.
- , C. M. PRINGLE, AND F. J. TRISKA. 1996. Nitrate reduction in sediments of lowland tropical streams draining swamp forest in Costa Rica: An ecosystem perspective. *Biogeochemistry* **33**: 179-196.
- , B. TONER, A. P. JACKMAN, R. J. AVANZINO, AND F. J. TRISKA. 1999. Determination of groundwater discharge into a sand and gravel bottom river: A comparison of chloride dilution and seepage meter techniques. *Verh. Int. Verein. Limnol.* **27**: 1-6.
- , AND F. J. TRISKA. 1990. Denitrification in sediments from the hyporheic zone adjacent to a small forested stream. *Can. J. Fish. Aquat. Sci.* **47**: 1140-1147.
- , AND ———. 2000. Nitrogen biogeochemistry and surface-subsurface exchange in streams, p. 197-220. *In* J. B. Jones and P. J. Mulholland [eds.], *Streams and ground waters*. Academic.
- , ———, J. W. HARVEY, A. P. JACKMAN, AND J. W. LABAUGH. 1997. The influence of streambed sediments on the solute chemistry of ground-water discharge in the upper Shingobee River, p. 143-147. *In* T. C. Winter [ed.], *Hydrological and biogeochemical research in the Shingobee River headwaters area, North-Central Minnesota*. U.S. Geological Survey, WRIR 96-4215.
- EMERSON, K., R. C. RUSSO, R. E. LUND, AND R. V. THURSTON. 1975. Aqueous ammonia equilibrium calculations: Effect of pH and temperature. *J. Fish. Res. Board Can.* **32**: 2379-2383.
- FIEBIG, D. M. 1992. Fates of dissolved free amino acids in ground-water discharged through stream-bed sediments. *Hydrobiologia* **235/236**: 311-319.
- , AND M. A. LOCK. 1991. Immobilization of dissolved organic carbon from groundwater discharging through the stream bed. *Freshw. Biol.* **26**: 45-55.
- GARCIA-RUIZ, R., S. H. PATTINSON, AND B. A. WHITTON. 1998. Kinetic parameters of denitrification in a river continuum. *Appl. Environ. Microb.* **64**: 2533-2538.
- GRIMM, N. B. 1996. Surface-subsurface interactions in streams, p. 625-646. *In* F. R. Hauer and G. A. Lamberti [eds.], *Methods in stream ecology*. Academic.
- , AND S. G. FISHER. 1984. Exchange between surface and interstitial water: Implications for stream metabolism and nutrient cycling. *Hydrobiologia* **111**: 219-228.
- HAKENKAMP, C. C., H. M. VALETT, AND A. J. BOULTON. 1993. Perspectives on the hyporheic zone: Integrating hydrology and biology. Concluding remarks. *J. North Am. Benthol. Soc.* **12**: 94-99.
- HENDRICKS, S. P. 1993. Microbial ecology of the hyporheic zone—a perspective integrating hydrology and biology. *J. North Am. Benthol. Soc.* **12**: 70-78.
- HYMAN, M. R., AND P. M. WOOD. 1985. Suicidal inactivation and labelling of ammonia mono-oxygenase by acetylene. *Biochem. J.* **227**: 719-725.
- HYNES, R. K., AND R. KNOWLES. 1978. Inhibition by acetylene of ammonia oxidation in *Nitrosomonas Europaea*. *FEMS Microbiol. Lett.* **4**: 319-321.
- , AND ———. 1980. Denitrification, nitrogen fixation and nitrification in continuous flow laboratory soil columns. *Can. J. Fish. Aquat. Sci.* **60**: 366-363.
- JACKMAN, A. P., J. H. DUFF, AND F. J. TRISKA. 1997. Hydrological examination of ground-water discharge into the upper Shingobee River, p. 137-142. *In* T. C. Winter [ed.], *Hydrological and biogeochemical research in the Shingobee River headwaters area, North-Central Minnesota*. U.S. Geological Survey, WRIR 96-4215.
- JENKINS, M. C., AND M. KEMP. 1984. The coupling of nitrification and denitrification in two estuarine sediments. *Limnol. Oceanogr.* **29**: 609-619.
- JENSEN, K., N. P. REVSBECH, AND L. P. NIELSEN. 1993. Microscale distribution of nitrification activity in sediment determined with a shielded microsensor for nitrate. *Appl. Environ. Microb.* **59**: 3287-3296.
- , N. P. SLOTH, N. RISGAARD-PETERSEN, S. RYSGAARD, AND N. P. REVSBECH. 1994. Estimation of nitrification and denitrification from microprofiles of oxygen and nitrate in model sediment systems. *Appl. Environ. Microb.* **60**: 2094-2100.
- JONES, J. B., S. G. FISHER, AND N. B. GRIMM. 1995. Nitrification in the hyporheic zone of a desert stream ecosystem. *J. North Am. Benthol. Soc.* **14**: 249-258.
- KASPAR, H. F. 1982. Denitrification in marine sediments: Measurement of capacity and estimate of in situ rate. *Appl. Environ. Microb.* **43**: 522-527.
- KEENEY, D. R., R. L. CHEN, AND D. A. GRAETZ. 1971. Importance of denitrification and nitrate reduction in sediments to the nitrogen budgets in lakes. *Nature* **233**: 66.
- , AND D. W. NELSON. 1982. Nitrogen-inorganic forms, p. 643-698. *In* A. L. Page [ed.], *Methods of soil analysis: Part 2. Chemical and microbiological properties*. Agronomy; no. 9. American Society of Agronomy, Soil Science Society of America.
- KELSO, B. H. L., R. V. SMITH, R. J. LAUGHLIN, AND S. D. LENNOX. 1997. Dissimilatory nitrate reduction in anaerobic sediments leading to river nitrite accumulation. *Appl. Environ. Microb.* **63**: 4679-4685.
- KEMP, M. J., AND W. K. DODDS. 2002. Comparisons of nitrification and denitrification in prairie and agriculturally influenced streams. *Ecol. Appl.* **12**: 998-1009.

- KILLHAM, K. 1994. Soil ecology. Cambridge Univ. Press.
- MARXSEN, J., AND D. M. FIEBIG. 1993. Use of perfused cores for evaluating extracellular enzyme activity in stream-bed sediments. *FEMS Microbiol. Ecol.* **13**: 1–12.
- MCCARTHY, J. J., W. R. TAYLOR, AND J. L. TAFT. 1977. Nitrogenous nutrition of the plankton in the Chesapeake Bay. I. Nutrient availability and phytoplankton preferences. *Limnol. Oceanogr.* **22**: 996–1011.
- MCLAREN, A. D. 1970. Temporal and vectorial reactions of nitrogen in soil: A review. *Can. J. Soil Sci.* **50**: 97–109.
- MISRA, C., D. R. NIELSEN, AND J. W. BIGGAR. 1974. Nitrogen transformations in a soil during leaching: II. Steady state nitrification and nitrate reduction. *Soil Sci. Soc. Am. Proc.* **38**: 294–299.
- MULHOLLAND, P. J., E. R. MARZOLF, J. R. WEBSTER, D. R. HART, AND S. P. HENDRICKS. 1997. Evidence that hyporheic zones increase heterotrophic metabolism and phosphorus uptake in forest streams. *Limnol. Oceanogr.* **42**: 443–451.
- NIELSEN, L. P., AND R. N. GLUD. 1996. Denitrification in a coastal sediment measured in situ by the nitrogen isotope pairing technique applied to a benthic flux chamber. *Mar. Ecol. Prog. Ser.* **137**: 181–186.
- NISHIO, T., I. KOIKE, AND A. HATTORI. 1982. Denitrification, nitrate reduction, and oxygen consumption in coastal and estuarine sediments. *Appl. Environ. Microb.* **43**: 648–653.
- PALMER, M. A. 1993. Experimentation in the hyporheic zone: Challenges and prospectus. *J. North Am. Benthol. Soc.* **12**: 84–93.
- PATRICK, W. H., AND K. R. REDDY. 1976. Nitrification-denitrification reactions in flooded soils and water bottoms: Dependence on oxygen supply and ammonium diffusion. *J. Environ. Qual.* **5**: 469–472.
- RICE, C. W., AND J. M. TIEDJE. 1989. Regulation of nitrate assimilation by ammonium in soils and in isolated soil microorganisms. *Soil. Biol. Biochem.* **21**: 597–602.
- RYSGAARD, S., N. RYSGAARD-PETERSEN, N. P. SLOTH, K. JENSEN, AND L. P. NIELSEN. 1994. Oxygen regulation of nitrification and denitrification in sediments. *Limnol. Oceanogr.* **39**: 1643–1652.
- SAIN, P., J. B. ROBINSON, W. N. STAMMERS, N. K. KAUSHIK, AND H. R. WHITELEY. 1977. A laboratory study of the role of stream sediment in nitrogen loss from water. *J. Environ. Qual.* **6**: 274–278.
- SHEIBLEY, R. W., A. P. JACKMAN, J. H. DUFF, AND F. J. TRISKA. In press. Numerical modeling of coupled nitrification-denitrification in sediment perfusion cores from the hyporheic zone of the Shingobee River, MN. *Adv. Water Resour.*
- SLOTH, N. P., L. P. NIELSEN, AND H. BLACKBURN. 1992. Nitrification in sediment cores measured with acetylene inhibition. *Limnol. Oceanogr.* **37**: 1108–1112.
- SORENSEN, J. 1978a. Capacity for denitrification and reduction of nitrate to ammonia in coastal marine sediment. *Appl. Environ. Microb.* **35**: 301–305.
- . 1978b. Denitrification rates in a marine sediment as measured by the acetylene inhibition technique. *Appl. Environ. Microb.* **36**: 139–143.
- STAMMERS, W. N., J. B. ROBINSON, H. R. WHITELEY, AND N. K. KAUSHIK. 1983. Characterization of the kinetics of “denitrification” in stream sediments, p. 479–486. *In* T. D. Fontaine and S. M. Bartell [eds.], *Dynamics of lotic systems*. Ann Arbor Science.
- STRAUSS, E. A., AND G. A. LAMBERTI. 2000. Regulation of nitrification in aquatic sediments by organic carbon. *Limnol. Oceanogr.* **45**: 1854–1859.
- TIEDJE, J. M., J. SORENSEN, AND Y.-Y. L. CHANG. 1981. Assimilatory and dissimilatory nitrate reduction: Perspectives and methodology for simultaneous measurement of several nitrogen cycle processes, p. 331–342. *In* F. E. Clark and T. Rosswall [eds.], *Terrestrial nitrogen cycles*. Ecological Bulletin.
- TRISKA, F. J., J. H. DUFF, AND R. J. AVANZINO. 1993a. Patterns of hydrological exchange and nutrient transformation in the hyporheic zone of a gravel-bottom stream—examining terrestrial aquatic linkages. *Freshw. Biol.* **29**: 259–274.
- . 1993b. The role of water exchange between a stream channel and its hyporheic zone in nitrogen cycling at the terrestrial-aquatic interface. *Hydrobiologia* **251**: 167–184.
- , V. C. KENNEDY, R. J. AVANZINO, G. W. ZELLWEGER, AND K. E. BENCALA. 1989. Retention and transport of nutrients in a third-order stream in northwestern California: Channel processes. *Ecology* **70**: 1877–1892.
- TURNER, R. E., AND N. N. RABALAIS. 1994. Coastal eutrophication near the Mississippi river delta. *Nature* **368**: 619.
- WEISS, R. F., AND B. A. PRICE. 1980. Nitrous oxide solubility in water and seawater. *Mar. Chem.* **8**: 347–359.
- WINTER, T. C., J. W. HARVEY, O. L. FRANKE, AND W. M. ALLEY. 1998. Ground water and surface water A single resource. U.S. Geological Survey, 1139.
- YOSHINARI, T., AND R. KNOWLES. 1976. Acetylene inhibition of nitrous oxide reduction by denitrifying bacteria. *Biochem. Biophys. Res.* **69**: 705–710.

Received: 4 May 2002

Accepted: 30 December 2002

Amended: 1 February 2003